Phenomenology of quasifree scattering

C. Kalbach
Physics Department, Duke University, Durham, North Carolina 27706
(Received 2 November 1989)

The systematics of quasifree scattering have been studied and parametrized for incident proton energies of 100–1000 MeV on a variety of targets. The observed position of the quasifree scattering peak at various emission angles closely tracks the kinematics for free nucleon-nucleon scattering. The peak widths are a function of the incident energy and of $\sin\theta$ in the N-N center of mass. The angle-integrated cross section is described in terms of a peripheral interaction with a single nucleon in the target nucleus and has a threshold of 150–200 MeV. The angular variation of the cross section is either nearly isotropic or, at higher energies, exponential in $\cos\theta$. The simple parametrization derived here allows a semiquantitative estimate of quasifree scattering peaks with no adjustable parameters.

I. INTRODUCTION

Work on the systematics of continuum angular distributions[1] resulted in a universal description of the angular dependence of the cross section from compound nucleus, preequilibrium, and direct nucleon transfer reactions. Alpha-particle knockout may also be included, but several reaction mechanisms were identified as showing remarkably different behavior. They are fragmentation of complex projectiles, strong collective excitations such as giant resonances, and quasifree scattering of nucleons. The present work represents an effort to uncover and describe the systematics of quasifree scattering through an appeal to data available in the literature.

For the purpose of this work, the term *quasifree scattering* refers to reactions in which an incident nucleon scatters off of a single nucleon in the target, essentially as if the rest of the nucleus were not there. Thus its experimental signature is a peak in the double-differential cross section that closely follows the kinematics for free nucleon-nucleon scattering.

Past work on quasifree scattering (QFS) generally followed one of two tracks. Many calculations[2–7] have been done using the impulse approximation or the distorted-wave impulse approximation (DWIA), perhaps with a theoretical estimate of the effective number of nucleons available for QFS, and a more or less realistic momentum distribution for the target nucleons. Typically, the momentum distribution was a particular focus of the work. Most often, no subtraction of background underneath the experimental QFS peak was made.

Another set of papers,[8–11] mainly concentrating on incident energies below 300 MeV, was aimed at studying giant-resonance states in the continuum. For this work, QFS plus any other non-giant-resonance strength constitutes a background which has sometimes been fit in an *ad hoc* way using several free parameters. One paper[12] used QFS to make estimates of the nucleon mean free path in a nucleus.

As new applications require extending the utility of preequilibrium reaction models to energies of 100–200 MeV, the QFS process must be accounted for. Thus there is a need for a simple method of describing it which can be incorporated into general reaction codes based on the Hauser-Feshbach model. Yet none of the work just mentioned produces the kind of very simple universal prescription of quasifree scattering which is needed for applied work. The present work was designed to arrive at such a prescription.

In addition, a general phenomenological prescription of QFS should be useful in subtracting QFS strength in future giant-resonance studies. Finally, it is hoped that this work will encourage the use of background subtraction in studies using QFS to gain information about momentum distributions inside the nucleus.

This work intentionally deals only with the energy and angular distributions of the QFS strength. A very limited amount of analyzing power data are available,[9,10] but even in the region of the QFS peak it almost certainly includes some additional non-giant-resonance strength. (This could, perhaps, explain the observation[9] that the analyzing power in this region follows the general trends of but is somewhat lower than the corresponding results for free scattering.) In addition, analyzing powers are not needed in the applications envisioned for this work.

The general strategy employed here is the one that worked well in studies of the systematics of continuum angular distributions.[1,13] First, a data set is assembled from the literature and studied to determine the systematics of the process under investigation (in the present case how the QFS peak depends on the important reaction variables). Then a simple parametric form is sought that is physically reasonable and that permits the description of the observed systematics with a small number of global parameter values.

Section II of this report describes the method used in greater detail, Sec. III presents the systematic behavior observed, and Sec. IV gives its parametrization. Section V compares the QFS peaks calculated from the current phenomenological description with the original data, and Sec. VI summarizes the conclusions of the work.

II. STUDYING THE DATA

In the present work it was decided to study data over the entire range of incident energies from 100 to 1000 MeV. Since the QFS peaks are generally clearer at the higher bombarding energies, the high-energy data can then be used to establish baseline systematics which, in turn, can guide the interpretation of the 100–300-MeV data where collective states can interfere.

A. The data

A set of over 100 (p,p') and (p,n) energy spectra[2,4,8,14–20] taken at forward angles (generally 30° or less in the laboratory) has been assembled. All exhibit peaks at roughly the energy predicted for free nucleon-nucleon (N-N) scattering and most are part of data systems in which the tracking of peak energy with emission angle can be verified. Table I summarizes the data.

B. Isolating the QFS cross section

The first step in the analysis was to plot all of these spectra in a consistent way and to subtract the "background" underneath the QFS peak. Here the background is the cross section usually of interest in preequilibrium reaction studies. Its size was generally estimated from the trends of the continuum at lower and, where possible, higher emission energies. A few of the spectra are fragmentary and do not cover a wide enough range of emission energies to estimate the underlying cross section very well. In these cases, guidance from spectra on other targets or at neighboring angles was generally available.

The biggest difficulty in isolating the QFS cross section occurred at 100–200 MeV where giant-resonance strength is prominent in the region of the spectrum where QFS strength should occur.

At 100 MeV this problem was surmounted by appealing to the general angular distribution systematics of Ref. 1. The data[14] exhibit a broad, flat-topped bump at 8°, 10°, 15°, and perhaps 25°. This bump has previously been interpreted as due to QFS (Ref. 14) and, indeed, seems to shift down slightly in energy with increasing emission angle. On the other hand, the data of Ref. 21 from the same laboratory can be combined with the systematics of Ref. 1 to estimate the cross section underlying the bump. The remaining cross section is then seen to occupy a fixed location in the spectrum between about 55 and 85 MeV in the laboratory and to disappear totally at 25°. Thus the bump seems not to be due to quasifree scattering (a small QFS contribution cannot be ruled out) but is most likely due to giant-resonance excitation.

The 200-MeV (p,p') data[15] are more difficult to deal with. First, the published data at forward angles are given only as counts, not cross sections. Additional graphs[22] (supplied for the work of Ref. 1) give cross-section values but include only two of the forward angles. A rough normalization of the published "counts" data was accomplished by demanding a smooth behavior of the cross section with angle at an emission energy of 40 MeV. The range of data at larger angles was not sufficient to allow the use of the angular distribution systematics as an effective means of isolating the extra for-

TABLE I. Data used to study systematics.

Reaction	Inc. energy (MeV)	Targets	Laboratory emission angles (deg)	Reference
(p,p')	100	Ni	8,10,15,25	14
	200	^{27}Al	14,17,20,25,30	15
	300	^{206}Pb	20	16
	400	^{12}C,^{58}Ni,^{206}Pb	16,30	16
		^{58}Ni	16,20,25,30	16
		^{206}Pb	16,20,30	16
	500	^{206}Pb	16	16
	450[a]	Be,C,Al	30	17
	558	Be,C,Al,Fe,Ge, W,Pb	10,20,30,40	18
	660	Be,C,Cu,U	12.2,18,24,30	2
	795	^{12}C,^{27}Al,^{40}Ca, ^{51}V,^{90}Zr,^{208}Pb	11,13,15,20,25, 30	4
	1014	^{12}C,^{40}Ca	9,11,13.5,15.1, 17.2,20.2	19
(p,n)	200[b]	^{90}Zr	7,9.5,19	8
		^{208}Pb	9.5,13,14.5,19	8
	318	Be,C	7.5,30	20
		Al,Ni,Ta,W,Pb,U	7.5	20
	450[a]	C	20,30	17
		Al,Co	20	17
	800	Al,Pb,U	7.5	20

[a]Weak data set used only to estimate magnitude of σ_{QFS}.
[b]No absolute normalization. Spectral shapes only.

ward angle cross section, so the general method of extending the continuum under the high-energy peaks was used. The remaining cross section was provisionally assumed to be QFS except for a sharper, narrower peak due to the known giant quadrupole resonance at an emission energy close to 180 MeV. Additional giant-resonance strength could also be present, but when an estimate of the giant quadrupole resonance (GQR) strength is removed from consideration, the remaining cross section forms a peak of reasonable width for QFS and its position shifts in a roughly appropriate way with angle.

Some 200-MeV (p,n) data[8] were also considered. These include only the upper third of the energy spectrum, and do not have any absolute normalization. They also contain large contributions from the isobaric analog state, the Gamov-Teller resonance, and a giant $L=1$ resonance. The data forward of 5° were totally dominated by these states. For the 7°, 9.5°, and 12.8° spectra, a significant fraction of the cross section in the prominent bump might be due to QFS. Thus these spectra were retained only for the purpose of extracting limits on the peak positions and widths of any QFS strength present.

The 300-MeV (p,p') data[16] and the 318-MeV (p,n) data[20] were analyzed assuming the broad high-energy peak in each spectrum is QFS, but bearing in mind that, especially at the most forward angles, it could contain significant collective strength.

Finally, it should be mentioned that for the 558-MeV (p,p') data[18], the energy resolution in the region of the QFS peak is fairly poor, especially at 10° and 20°. Thus the elastic scattering peak is completely unresolved and will contribute to the designated QFS peak. This is particularly a problem at 10°.

C. Characterizing the quasifree scattering strength

One the QFS strength was isolated, several pieces of data were extracted from each peak. The laboratory emission energy at the maximum of the distribution was determined and designated as the peak energy E_0. Next the peak widths were characterized by measuring the half-widths at half-maximum (HWHM) for both the low- and high-energy half-peaks. For some spectra, the elastic scattering peak obscured the upper part of the QFS distribution so that only the low-energy width could be estimated. Finally, each half-peak for which an absolute normalization was available was integrated to get an estimate of the angle-differential cross section $d\sigma/d\Omega$. For those spectra in which the upper half of the peak was obscured by elastic scattering or giant-resonance strength, the cross section in that half was later estimated from the lower half-peak and the peak-width systematics.

In some cases, the quoted experimental energy resolution is significant relative to the width of the QFS distribution. In these cases, the measured peak widths were corrected, assuming that the real and instrumental widths add in quadrature. Typically this was only an issue at the most forward angles and only for a few systems.

III. OBSERVED SYSTEMATICS

Because of the difficulties in subtracting the background under the QFS peaks and in some cases because of the uncertainties inherent in the data themselves, the estimates of peak energies, widths, and cross sections extracted above often have significant uncertainties associated with them. As a result only first-order systematics can be extracted. The uncertainties were particularly large at the lower bombarding energies (≤ 300 MeV) where giant-resonance states can interfere. For some parameters the uncertainties could be reduced by averaging results over target mass or emission angle as noted below.

A. Systematics of the peak energies

The QFS peak positions were found not to vary significantly or systematically with target mass. Thus for data sets which include multiple targets, the peak energies for each laboratory angle were averaged. These averaged energies are shown in Fig. 1 for (p,p') QFS at several incident energies and can be seen to represent a shift from the energy for free N-N scattering that is nearly invariant with angle.

Figure 2 shows this energy shift averaged over emission angle as a function of incident energy. A striking result here is the difference between the (p,p') and (p,n) reactions. For incident energies at or above 400 MeV the (p,p') QFS peaks are essentially at the free scattering energies while the (p,n) peaks are shifted down in laboratory energy by some 40 MeV. At lower incident energies the peak energies for the two reactions seem to converge, though the trend in the (p,n) case is only very weakly defined.

B. Systematics of the peak widths

Like the peak positions, the peak widths show no systematic or significant variation with target mass, so again values for multiple targets were averaged. Further, since it is desired to describe the QFS peaks as the combination of two half-Gaussians, the HWHM values were multi-

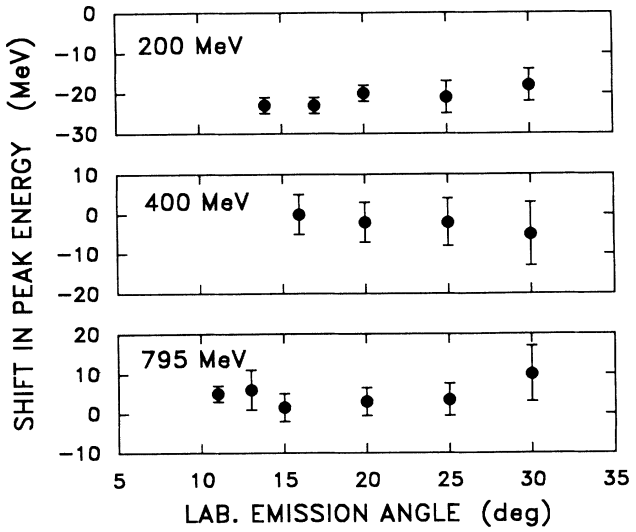

FIG. 1. Experimental (p,p') QFS peak energies averaged over target mass as a function of laboratory emission angle for the three designated incident energies.

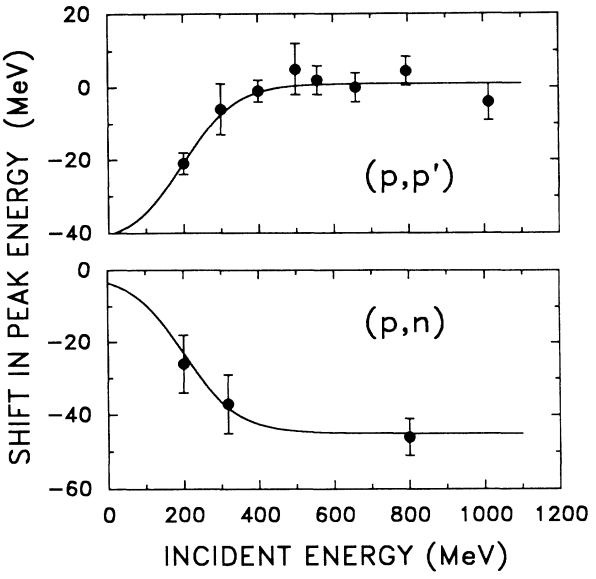

FIG. 2. Experimental QFS peak energies averaged over target mass and emission angle shown as a function of incident energy. The curves show the adopted systematics.

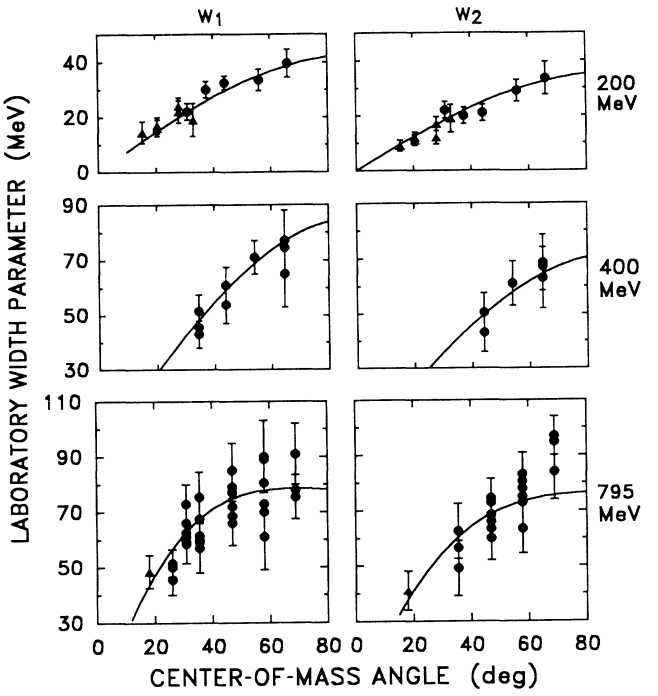

FIG. 3. Experimental laboratory peak width parameters, w_1 and w_2, shown as a function of the center-of-mass emission angle for the three designated incident energies. Circles give the results for (p,p') QFS while triangles give the results for (p,n). The curves show the adopted systematics.

plied by 1.20 to convert them into Gaussian width parameters (i.e., half-widths at $1/e$ of peak intensity). These have been designated w_1 and w_2 for the low- and high-energy half-peaks, respectively.

Figure 3 shows the w_i values as a function of the emission angle θ_c in the N-N center of mass for a few representative bombarding energies. Both w_1 and w_2 increase with increasing emission angle, at least initially, and their trends are consistent with zero widths at 0°, though no experimental values were obtained for angles less than $\theta_c = 15°$. It might also be expected that the laboratory widths would tend toward zero at 180° in the N-N center of mass. Indeed it looks from Fig. 3 as if the width distribution is starting to level out just below 90°, and at the highest incident energies they seem to turn over even at angles as small as 40°. Reasonable lower limits on the widths are discussed in connection with the parametrization.

It is also significant that the peak widths for (p,p') and (p,n) quasifree scattering are quite comparable in spite of the differences in their peak positions. On the other hand, there are noticeable differences between w_1 and w_2, with the low-energy width parameter tending to be slightly larger than its high-energy counterpart except at the highest incident energies.

C. Mass dependence of the QFS cross section

The quasifree scattering process is generally assumed to occur in peripheral nuclear collisions. Thus the cross section should vary roughly as $A^{1/3}$, the cube root of the target mass.

For (p,p') reactions the $d\sigma/d\Omega$ values extracted from the data at a given incident energy and emission angle have been fit with an A^n dependence, and values of n were extracted from log-log plots of $d\sigma/d\Omega$ vs a. These values are given in Table II and can be seen to cluster around $n = \frac{1}{3}$. Further there is no convincing dependence of this value on emission angle.

For (p,n) reactions the dependence is not as simple because the projectile must strike a neutron in the target. Thus the cross section would be expected to be reduced roughly by a factor of N/A, where N is the neutron number of the target. Plots of $(A/N)\, d\sigma/d\Omega$ vs A yield the values of n shown in Table II. The value at 318 MeV is still quite high, probably indicating the importance of giant-resonance processes, but at 800 MeV the value is consistent with the results for (p,p') quasifree scattering.

(A similar modification for (p,p') QFS would produce an extra factor of the form $[(1+f)Z+N]/A$, where f is the ratio of the probabilities for the struck and incident nucleons to be emitted. As discussed later in this paper, the values of f appear to be less than 1, but even with $f=1$ this factor would produce too small an effect to be observed in the present study.)

D. Angle dependence of the QFS cross section

The angular dependence of the quasifree scattering cross section was studied by converting the integrated cross sections from the laboratory to the N-N center-of-mass system. Only for the (p,p') reaction were the data complete enough for this investigation. Because of the consistency of the observed target dependence and because of the uncertainties in individual peak intensities, the results from multiple targets were combined assuming

TABLE II. Mass dependence of QFS cross section.

Reaction	E_{inc} (MeV)	θ_l (deg)	n [a]	m [b]
(p,p')	400	16	0.30±0.02	
	558	20	0.34±0.04	
		30	0.37±0.03	
	660	12.2	0.34±0.03	
		18	0.38±0.02	
		24	0.38±0.05	
		30	0.38±0.05	
	795	11	0.33±0.04	
		13	0.32±0.02	
		15	0.35±0.02	
		20	0.32±0.02	
(p,n)	318	7.5	0.75±0.05[c]	0.64±0.04[c]
	800	7.5	0.41±0.03	0.34±0.03

[a]From $d\sigma/d\Omega \propto A^n$.
[b]From $d\sigma/d\Omega \propto (N/A)A^m$.
[c]Be and C targets not included in the fit.

an $A^{1/3}$ dependence on target mass.

Guided by the general systematics of Ref. 1, the cross sections were plotted on a semilogarithmic scale vs $\cos\theta_c$. The results were consistent with an exponential falloff in cross section with $\cos\theta_c$ but with the (p,p') data at 200 to 400 MeV being isotropic to within the error bars. Slope parameters for the exponential decay of cross section with center-of-mass emission angle are shown in Fig. 4.

It should, however, be emphasized that the angle range of the data is quite limited, extending roughly from 15° to 80° in the N-N center of mass. Thus it is possible that there could be a turn down in the cross section at more forward angles due to Pauli blocking at small momentum transfers and that there could be a rise at more backward angles mirroring that seen in free scattering.

E. Total QFS cross sections

The total quasifree scattering cross sections were estimated from the $d\sigma/d\Omega$ values by assuming an exponential falloff of the cross section in $\cos\theta_c$ and using slope parameters obtained from the parametrization described in Sec. IV. The results, scaled to a ^{58}Ni target and averaged over multiple targets prior to angle integration, are shown in Fig. 5.

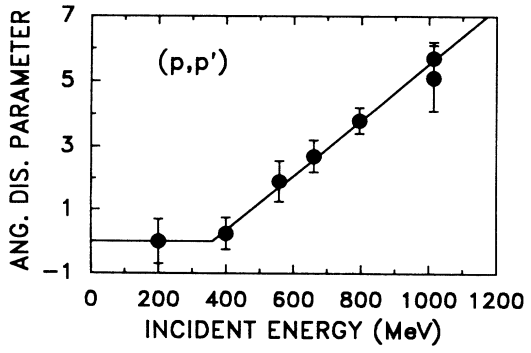

FIG. 4. Empirical angular distribution slope parameters for (p,p') quasifree scattering as a function of the incident energy. The lines give the results from the adopted parametrization.

These empirical values can be compared with the corresponding free-scattering cross sections in order to determine an average effective number of nucleons in the target nucleus. Such a comparison is given in Table III where the effective N-N cross sections were taken to be $\langle\sigma_{NN}\rangle=(2\sigma_{pp}+\sigma_{pn})/2$ for (p,p') QFS and $\langle\sigma_{NN}\rangle=\sigma_{pn}/2$ for (p,n).

The results of Table III indicate that a ^{58}Ni target has a QFS cross section that is one to five times the size of the average free-scattering cross section. For other targets, this number should scale roughly as $A^{1/3}$ for (p,p') or $(N/A)\,A^{1/3}$ for (p,n).

IV. PARAMETRIZATION OF THE SYSTEMATICS

Equations have been sought which would simply but faithfully reproduce the observed systematics of the

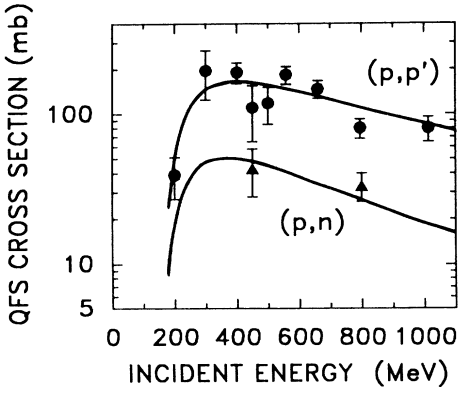

FIG. 5. Total QFS cross section evaluated for a ^{58}Ni target shown as a function of the incident energy. The experimental points represent the combined results for all targets scaled to ^{58}Ni. The curves show the results from the adopted parametrization.

TABLE III. Effective number of target nucleons in QFS on ^{58}Ni.

E_{inc} (MeV)	$\sigma_{QFS}(p,p')$ (mb)	$\sigma_{QFS}(p,n)$ (mb)	$\sigma_{QFS}/\langle\sigma_{NN}\rangle$ (p,p')	(p,n)
200	39±12		0.9	
300	195±50		4.9	
400	192±30		5.1	
450	106±40	43±8	2.9	2.9
558	185±25		5.2	
660	147±20		4.3	
795	79±10	33±7	2.4	3.2
1014	80±15		2.6	

quasifree scattering peaks in nucleon-nucleon reactions. Where possible, the form of the assumed dependence was guided by physical considerations, but the resulting equations can in no sense be considered as either unique or theoretically based. They should, however, be physically reasonable.

In earlier work on angular distributions[1] it was possible to use only a subset of the data for the parametrization process. This permitted an excellent check of the predictive ability of the parametrization through its application to the full data set. In the present case this procedure was not followed because of the added scatter in the data produced largely by the background subtraction process. Thus, target averaging is important. In addition, the data are somewhat sparcely distributed in incident energy. Thus the full data set is utilized in the parametrization process.

A. Peak positions

The energies of the quasifree scattering peaks have been referenced to the energy of the corresponding free-scattering peak. This peak energy follows the relativistic relationship

$$E_f(E_{inc},\theta_1)=\frac{E_{inc}\cos^2\theta_1}{1+(E_{inc}/2M)\sin^2\theta_1}\ , \tag{1}$$

where M is the rest mass of a nucleon or 939 MeV and θ_1 is the laboratory emission angle. In terms of this free-scattering energy, the peak energies in the laboratory system can be described by the equations

$$E_0^{(p,p')}(E_{inc},\theta_1)=E_f(E_{inc},\theta_1)-43+\frac{44}{1+\exp[(200-E_{inc})/70]}\ , \tag{2}$$

$$E_0^{(p,n)}(E_{inc},\theta_1)=E_f(E_{inc},\theta_1)-1-\frac{44}{1+\exp[(200-E_{inc})/70]}\ , \tag{3}$$

where it is assumed that all energies are given in MeV. The values calculated using Eqs. (2) and (3) are given in Fig. 2 along with the empirical values for E_0.

B. Peak widths

It turns out to be convenient to describe the two width parameters in terms of the cosine of the emission angle in the N-N center of mass, where this angle is calculated relativistically. The pertinent equations for determining θ_c are

$$\cot\theta_c=\gamma\cot\theta_1-\left[\frac{D_{al}R}{D_{bl}}\right]^{1/2}\gamma\gamma_{bl}\csc\theta_1\ , \tag{4}$$

$$D_{al}=E_{inc}(\gamma_{al}+1)\ , \tag{5}$$

$$\gamma_{al}=1+E_{inc}/M\ , \tag{6}$$

$$D_{bl}=E_0(\theta_l)(\gamma_{bl}+1)\ , \tag{7}$$

$$\gamma_{bl}=1+E_0(\theta_l)/M\ , \tag{8}$$

$$\gamma=\left[\frac{E_{inc}+2M}{2M}\right]^{1/2}\ , \tag{9}$$

$$R=(\gamma_{al}+1)^{-2}\ . \tag{10}$$

In terms of the angle θ_c, the width parameters w_1 and w_2 are given by the relations

$$w_1=\frac{E_{inc}}{4.7}\sin\theta_c-\frac{E_{inc}-540}{2.8}\sin^2\theta_c\Theta(E_{inc}-540)\ , \tag{11}$$

$$w_2=\text{minimum}\ (w_{2a},w_{2b})\ , \tag{12}$$

$$w_{2a}=\frac{E_{inc}}{5.6}\sin\theta_c-\frac{E_{inc}-540}{3.9}\sin^2\theta_c\Theta(E_{inc}-540)\ , \tag{13}$$

$$w_{2b}=\tfrac{2}{3}[E_{inc}-E_0(\theta_1)]\ . \tag{14}$$

Here Θ is the Heaviside function which is zero for a negative argument and one for a positive one. The extra condition of w_{2b} imposed on the high-energy width is designed to keep significant amounts of calculated QFS strength from falling above the physical end point of the spectrum. Technically speaking this end point should be shifted for (p,n) reactions due to Q-value effects, but in practice the (p,n) peaks are low enough in the spectrum that this limit is irrelevant. Possible modifications to Eqs. (11)–(14) for very small forward angles are considered later in this section.

C. Angular distributions

The QFS cross section is assumed to fall exponentially with the cosine of the emission angle in the N-N center of

mass. Thus the angle-differential cross section is given by

$$\frac{d\sigma(\theta_c)}{d\Omega_c}=\frac{a}{2\pi}\sigma_{\rm QFS}(E_{\rm inc},A,Z)\frac{\exp(a\cos\theta_c)}{e^a-e^{-a}}\ , \quad (15)$$

where $\sigma_{\rm QFS}$ is the total QFS cross section at the appropriate incident energy and on a target of mass number A and atomic number Z. The quantity a is the angular-distribution slope parameter estimated from the (p,p') data and has been parametrized as

$$a(E_{\rm inc})=0.086(E_{\rm inc}-360)\Theta(E_{\rm inc}-360)\ . \quad (16)$$

Thus $a=0$ for incident energies below 360 MeV so the angular distributions are isotropic in the N-N center of mass and $d\sigma/d\Omega=\sigma_{\rm QFS}/4\pi$. The parameter values obtained from Eq. (16) are shown in Fig. 4 along with the empirical values.

The angle-differential cross sections of Eq. (15) can be converted into the laboratory system using the relativistic equation

$$\frac{d\sigma(\theta_l)}{d\Omega_l}=\frac{d\sigma(\theta_c)}{d\Omega_c}\left[\frac{2D_{bl}}{E_{\rm inc}}\right]^{1/2}\frac{1}{\gamma}\times\left[1-\left[\frac{D_{al}R}{D_{bl}}\right]^{1/2}\gamma_{bl}\cos\theta_l\right]^{-1}\ . \quad (17)$$

D. Free nucleon-nucleon scattering cross sections

The parametrization of the quasifree scattering cross section is to be given in terms of the free nucleon-nucleon scattering cross sections. Thus it is useful to have simple equations describing these latter quantities. The present equations were derived starting from a parametrization[23] developed for intranuclear cascade model calculations. The N-N data of Ref. 23 were supplemented by the more recent tabulated values from Ref. 24.

For p-p data the new formula valid from 20 to 2000 MeV in the laboratory system is

$$\sigma_{pp}(E)=-\frac{1.69\times10^6}{E^3}+\frac{1.49\times10^5}{E^2}-\frac{692}{E}+22.4+\frac{E}{400}-\frac{E^2}{5\times10^5}\ , \quad (18)$$

where E is the laboratory energy of a proton incident on a stationary target. The p-n results are a bit more difficult since the data are sparce and have larger uncertainties. The new equation adopted is

$$\sigma_{pn}(E)=\frac{2.39\times10^5}{E^2}+\frac{1800}{E}+27.2-\frac{E-300}{50}\Theta(E-300)+\frac{(E-500)^2}{1.1\times10^5}\Theta(E-500)\ , \quad (19)$$

where, again, all energies are assumed to be given in MeV.

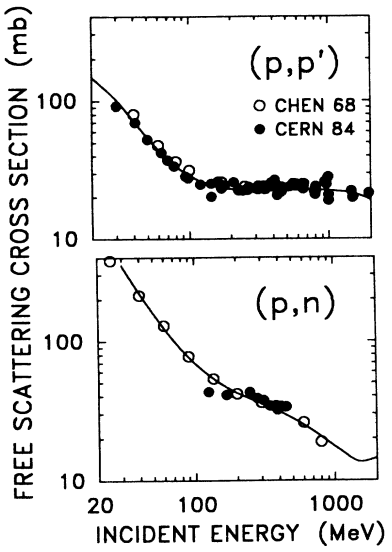

FIG. 6. Free nucleon-nucleon elastic scattering cross sections as a function of the incident energy. The points are the experimental values quoted in Refs. 23 and 24. The curves were generated by the adopted empirical equations.

Figure 6 shows a comparison of the results of Eqs. (18) and (19) with empirical values of the free p-p and p-n elastic cross section. For purposes of this work the standard assumption $\sigma_{nn}(E)=\sigma_{pp}(E)$ will be made.

E. The total QFS cross section

The total QFS cross section $\sigma_{\rm QFS}(E_{\rm inc},A,Z)$, as a function of the incident energy and the target nucleus, is the final piece of information needed. It is here thought of as the product of three terms,

$$\sigma_{\rm QFS}(E_{\rm inc},A,Z)=(\text{No. of target nucleons in active zone})\times(\text{probability that an interaction is with 1 nucleon})\times(\text{avg. free } N\text{-}N \text{ cross section})\ . \quad (20)$$

These terms are estimated using simple classical ideas. The logic is most clearly seen by starting with the third factor and working backwards.

The third term is an appropriate average over the p-p and p-n free-scattering cross sections, bearing in mind that one or both of the participating nucleons may be emitted. For (p,p') QFS it has the form

$$\langle\sigma_{NN}^{(p,p')}(E_{\rm inc},A,Z)\rangle=\frac{(1+f)Z\sigma_{pp}(E_{\rm inc})+N\sigma_{pn}(E_{\rm inc})}{A}\ , \quad (21)$$

while for (p,n) QFS it is

$$\langle \sigma_{NN}^{(p,n)}(E_{\rm inc}, A, Z)\rangle = \frac{fN\sigma_{pn}(E_{\rm inc})}{A} \ . \tag{22}$$

The free parameter f is the probability of the struck target nucleon being emitted relative to that for the incident nucleon being reemitted, and it adjusts the relative magnitudes of the (p,p') and (p,n) QFS cross sections. The quantity f is here assumed to be independent of emission angle and bombarding energy, a point which is commented upon later. It is also tentatively assumed that $\langle \sigma_{NN}^{(n,n')}\rangle$ and $\langle \sigma_{NN}^{(n,p)}\rangle$ are given by relations analogous to Eqs. (21) and (22) obtained by interchanging the roles of protons and neutrons.

The second factor is estimated by assigning an effective radius of r_a to the projectile and of r_t to a nucleon in the active zone of the target nucleus. The quantity r_a has the form

$$r_a = [(0.76\ \text{fm})^2 + (\lambda/2)^2]^{1/2} \ , \tag{23}$$

where λ is the de Broglie wavelength of the nucleon and 0.76 fm is the rms charge radius of the proton.[25] Similarly, r_t is given by

$$r_t = r_0(\rho_0/\rho)^{1/3} \ , \tag{24}$$

where ρ and ρ_0 are the local and central nucleon densities, and r_0 is the nuclear radius parameter, here taken to be 1.07 fm. Thus r_t is a measure of the space assigned to the target nucleon. Clearly, if $r_a > r_t$, then any interaction of the projectile will intrude into the space of another target nucleon and a simple QFS process will not occur. In a simple two-dimensional model, the probability that a target-projectile interaction will involve only one target nucleon can be estimated to be $[1-(r_a/r_t)]^2$ for $r_a < r_t$ and zero otherwise. Thus with $\rho_0/\rho = 2$, the second factor becomes

$$(\text{probability that an interaction is with 1 nucleon}) = \left[1 - \frac{r_a}{1.26 r_0}\right]^2 \ . \tag{25}$$

The first factor in Eq. (20) is the number of target nucleons in the peripheral area of the target that contributes to the QFS cross section. It is comprised of an effective active volume multiplied by an average local nucleon density ρ which is again assumed to be half the central density of $\rho_0 = 0.17\ \text{fm}^{-3}$. The effective volume is a ring with a radius equal to the nuclear radius, and a width and thickness still to be determined. To reproduce the empirical energy dependence of $\sigma_{\rm QFS}$, both the width and the thickness of the active volume need to be proportional to λ. Since an overall normalization constant will be used, the active volume is assumed to be a ring extending from $r_0 A^{1/3} - \lambda/2$ to $r_0 A^{1/3} + \lambda/2$ and having a thickness of λ. The third factor thus becomes

$$(\text{No. of targets nucleons in active zone}) = 2\pi\lambda^2 r_0 A^{1/3}(\rho_0/2) \ . \tag{26}$$

Combining all of these factors and including the arbitrary normalization factor C produces the final equation for the full QFS cross section. This is

$$\sigma_{\rm QFS}(E_{\rm inc}, A, Z) = C 2\pi\lambda^2 r_0 A^{1/3} \frac{\rho_0}{2} \times \left[1 - \frac{r_a}{1.26 r_0}\right]^2 \langle \sigma_{NN}^{(a,b)}\rangle \ . \tag{27}$$

The factor of λ^2 in Eq. (27) arose from setting both the width and thickness of the active zone of the nucleus proportional to λ. This choice was made to fine tune the incident energy dependence at high energies but is not unreasonable. Other adjustments are the quantity $f = 0.64 \pm 0.03$, which occurs in $\langle \sigma_{NN}^{(a,b)}\rangle$ and alters the relative sizes of the (p,p') and (p,n) QFS cross sections, and $C = 19 \pm 4$, which is an overall normalization constant. The uncertainties quoted for f and C reflect only scatter in the data but not possible errors in the assumed forms of the equations or the other parameters. For instance, if f, the ratio of the probabilities for the struck and striking nucleons to be emitted, were allowed to vary with incident energy, then the need for the factor of λ^2 would be modified and it might be possible to use a constant thickness for the active zone of the nucleus. The radius parameter $r_0 = 1.07 \pm 0.02$ fm was constrained to be close to 1.1 fm, but small variations were considered in order to optimize the threshold behavior of the cross section.

An angular variation of f would be seen in different angular distribution systematics for (p,p') and (p,n) QFS. The available data do not allow a resolution of this question so a constant value of f is assumed, and the (p,p') slope parameters of Eq. (16) are assumed to apply to (p,n) reactions as well.

Figure 5 shows a comparison of the results of Eq. (27) for (p,p') and (p,n) quasifree scattering and the estimates from the data at various incident energies. The calculations were carried out for a ^{58}Ni target, while the experimental peak intensities were scaled to this target as described earlier.

F. Double-differential energy spectra

As mentioned in Sec. III B, the quasifree scattering peak at a given emission angle is described as the sum of two half-Gaussians with width parameters w_1 and w_2, and a peak position of E_0. The combined integral of the half-Gaussians is the angle-differential cross section $d\sigma/d\Omega$. Thus the double-differential QFS cross section is written as

$$\frac{d^2\sigma(E_l,\theta_l)}{dE_l d\Omega_l} = \frac{d\sigma(\theta_l)}{d\Omega_l} \frac{2}{(w_1+w_2)\pi^{1/2}} \times \exp\left[-\left[\frac{E_0-E_l}{w_i}\right]^2\right], \quad (28)$$

where E_l is the laboratory energy of the emitted particle. The width parameter is taken to be $w_i = w_1$ for E_l less than E_0 and $w_i = w_2$ for E_l greater than E_0. This asymmetric form seems to adequately account for the trends of the data.

G. Behavior at extreme forward angle

There are two potential difficulties with the above systematics at angles ($\theta_l < 7.5°$) forward of those covered in the main data set. The first is the zero angle limit of the peak-width parameters and the other is the possibility that Pauli blocking could cause the forward-angle cross sections to be lower than given by the general systematics. A new data set[26] for (p,n) reactions on ^{12}C at 800 MeV allows these questions to be investigated.

Good resolution data are available at 0°, 1°, 3°, 4°, 6°, and 9° in the laboratory, and there is no elastic scattering peak to contend with. Two strong discrete peaks are seen at $E_n > 760$ MeV, but below this at least part of a QFS peak can be discerned. These spectra have thus been analyzed to look primarily at the peak widths and the angular dependence of the QFS cross section.

First, however, the peak positions were estimated, both as a necessary prelude to determining the widths and as a check for consistency with the general systematics. Only at 9° could the actual summit of the peak be clearly observed. It has a position of 738±5 MeV, as compared with a predicted value of 727 MeV. For the other angles, use was made of the broad bump in each spectrum which results from pion production in a single N-N scattering. This bump should have an essentially constant shift of about 300 MeV relative to the QFS peak itself. Thus, by estimating the shift with angle of the pion production bump, the shift of the QFS peak relative to its position at 9° could also be estimated. In this way it is found that the QFS peak falls about 32 MeV below the free scattering energy, as opposed to the predicted shift of 45 MeV. Considering the uncertainties in the (p,n) systematics this is not unreasonable.

The QFS peak widths for the low-energy half-peaks were estimated and found to be nearly constant (to within the large uncertainties) at around 37 MeV. Thus it is clear that the widths do not go to zero at 0°. Rather it seems that they reach some minimum value as the angle decreases and then stay there. It is clear that such a minimum must be a function of the incident energy, since at lower bombarding energies w_1 values as low as 15 MeV have been observed. A value of

$$w_{1\,\min} = 1.2E_{\rm inc}^{1/2} \quad (29)$$

is consistent with all observations when the energies and widths are given in MeV. The limit on w_2 may be different, and from the remaining width data it should be no larger than

$$w_{2a\,\min} = 0.8E_{\rm inc}^{1/2} . \quad (30)$$

These two minimum values have been provisionally adopted. Note also that the minimum criterion of Eq. (30) is to be applied to w_{2a} of Eq. (13). The quantity w_2 may be smaller than $w_{2a\,\min}$ if the physical cutoff at the end of the spectrum is reached. (On the other hand, in the present case, the cutoff is inoperative.)

Integrated cross sections could be estimated only from the low-energy half-peaks. From 3° to 9° they were

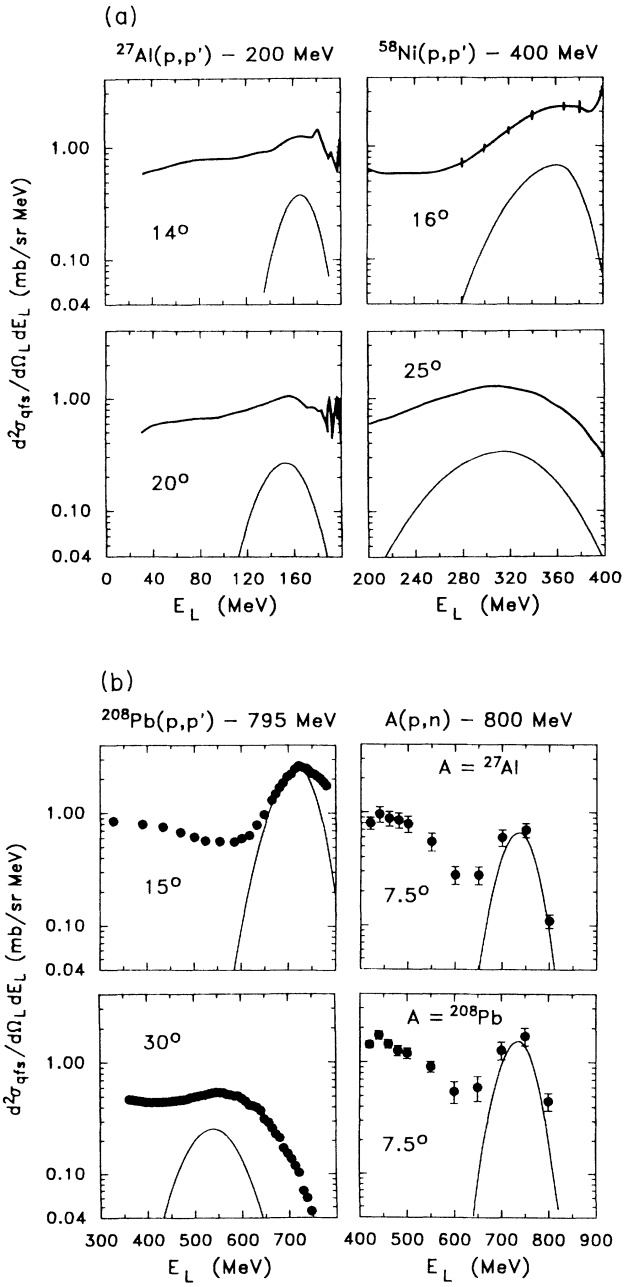

FIG. 7. Comparison between calculated QFS peaks and measured energy spectra for (p,p') reactions at 200, 400, and 795 MeV, and (p,n) reactions at 800 MeV. The thin curves give the calculated results while the data are indicated by thick curves or points.

TABLE IV. Additional data systems.

Reaction	Inc. energy (MeV)	Targets	Laboratory emission angles (deg)	Reference
(p,p')	150[a]	Be,C	20	12
	250	Si	6,10,13,17,21,25	11
	450[b]	Co,Bi	30	17
(p,n)	200[c]	Pb	4.5	8
	318[b]	Al,Ni,Ta,W,Pb,U	30	20
	450[b]	Al,Co	30	17
	800[b]	Al,Pb,U	30	20
	800	^{12}C	0,1,3,4,6,9	26

[a]The systematics predict no QFS.
[b]Minimal QFS visible in the data.
[c]No absolute normalization of the data.

found to be about 40% of the full-peak cross sections predicted by the systematics, while the 0° and 1° integrals are only about 20% of the predicted values. Since the energy transfers at the centers of the peaks are nearly the same at 1° and 3°, Pauli blocking does not seem to offer a ready explanation of the dramatic decrease in cross section at 0° and 1°. Nor is it possible from existing data to predict the size of this phenomenon at other incident energies or even for (p,p') reactions to 800 MeV. Clearly a lot more high-quality forward-angle data are needed to resolve these questions about peak widths and $d\sigma/d\Omega$.

V. COMPARISONS BETWEEN PARAMETRIZATION AND DATA

A simple FORTRAN code was written to calculate the QFS contribution to the experimental energy spectra using the equations given in this paper, and correcting for the instrumental resolution when this is significant relative to the width predicted for the QFS peak.

Calculations were performed for the data systems listed in Table I plus a few additional spectra.[8,11,12,17,20,26] The results for some of the original systems are shown in Fig. 7. The newer systems are listed in Table IV and, for the most part, represent spectra which were unsuitable for the original study because the QFS peak was either too small or too much obscured by other features in the spectrum. Thus their comparison with the systematics is more of a consistency check than a test of the model's predictive ability.

In general it is found that the parametrization does quite well at describing the general position and width of the QFS peaks. The intensities of the individual peaks are, for the most part, reproduced to better than a factor of 1.5. The level of agreement can thus be termed semiquantitative.

VI. SUMMARY AND CONCLUSIONS

This study has produced a useful description of nucleon-nucleon quasifree scattering, which is here defined as a process in which the incident nucleon scatters off of a target nucleon essentially as if the rest of the target were not there.

At incident energies at or above about 400 MeV the (p,p') QFS peak occurs at very nearly the energy calculated for free scattering, while the (p,n) QFS peak occurs 40 to 45 MeV below this energy. As the incident energy is decreased, the peaks for the two reactions seem to approach each other in energy. The peak energies can be parametrized using Eqs. (1)–(3).

The shape of the QFS peak is typically asymmetric with the low-energy side usually somewhat wider than the high-energy side. The width of the peak generally increases with increasing emission angle up to at least 50° in the N-N center of mass. There is preliminary evidence that at very small angles the width becomes constant at some minimum value that depends on incident energy. The general behavior of the widths has been parametrized in terms of the sine of the emission angle in the N-N center of mass using Eqs. (11)–(14). The minima are tentatively described by Eqs. (29) and (30).

The angular dependence of the QFS cross section is conveniently studied in the N-N center of mass where it is consistent with an exponential dependence of the type $\exp(a\cos\theta_c)$. The slope parameter a is roughly zero (indicating isotropy) for incident energies below about 400 MeV, and increases linearly with $E_{\rm inc}$ for higher bombarding energies, as described by Eq. (16). The range of angles for which these systematics are valid is typically 8° to 40° in the laboratory or 16° to 80° in the center of mass. The data of Ref. 26 indicate that at angles of less than 3° in the laboratory, at least for 800 MeV (p,n) reactions, the cross section drops below the predicted value. This phenomenon, which perhaps indicates an angle dependence of the parameter f, needs to be investigated further when more data become available. Also, it should be emphasized that at backward angles in the N-N center of mass the QFS peak is not seen in the data so that the angular dependence is unknown. The data are consistent with the present parametrization.

The angle-integrated, total QFS cross section shows a threshold of around 200 MeV and a maximum at 350 to 400 MeV which is followed by a slow falloff. For a ^{58}Ni target it has a magnitude which is roughly 1 to 5 times the corresponding free N-N elastic scattering cross section. It varies with the target roughly as $A^{1/3}$ for (p,p') and $(N/A)\,A^{1/3}$ for (p,n) reactions. The total QFS cross

section can be described by Eq. (27), with the average effective free-scattering cross sections given by Eqs. (21) and (22), (18), and (19).

Thus the peak positions and angular distribution parameter both undergo a kind of transition in their behavior for incident energies just below 400 MeV, the same energy domain at which the total QFS cross section reaches its maximum. This points to a significant change occurring at this energy, possibly related to the opening of inelastic channels in the free N-N cross section.

The current QFS parametrization is adequate to give at least a semiquantitative description of the observed QFS peaks once the underlying cross section has been subtracted. The peak positions are typically reproduced to within 5 MeV, the widths to within 10–20%, and the magnitude to within a factor of 1.5.

Since the present study used all of the cleanest data in the parametrization process, it is impossible to get a reliable estimate of its predictive ability. However, because of the global nature of the data base and because it represents results from many different laboratories, it is expected that the level of agreement found here would be typical for other systems in the mass-energy domain covered by this work. This was, indeed, the case in the work on preequilibrium angular distributions[1] where the predictive ability could be checked.

Additional (p,n) data are needed to firm up the QFS systematics for this reaction, and further work at very forward angles would be extremely useful. Even though these angles represent a very small part of the total angle-integrated cross section, they are often of great importance in practical applications and in the study of giant resonance phenomena. Finally, appropriate data for neutron induced QFS would be helpful.

The most useful data would be those that include a large number of forward angles, and a sufficient number of angles above 30° in the laboratory for the preequilibrium angular distribution systematics to be used in estimating the cross section underlying the QFS peak. Energy resolution sufficient to resolve and identify strong discrete features in the spectrum is important, though for purposes of studying the QFS strength, averaging in bins with a width of 1–2% of the incident energy is very useful.

Finally, it should be emphasized that while quasifree scattering in the sense meant here does not seem to occur for incident energies of 100 to 150 MeV and is thus not important for practical applications in this energy domain, there *will* be reaction contributions in this energy range in which there is a single N-N scattering.[27] The crucial difference is in the level of influence the remainder of the target nucleus has on the process.

ACKNOWLEDGMENTS

This work was performed under a consulting subcontract for Los Alamos National Laboratory and was funded by the U.S. Department of Energy. The author is grateful for the hospitality of the Duke University Physics Department and the Triangle Universities Nuclear Laboratory. Thanks also go to Dr. Michael Bozoian for a critical reading of this manuscript.

[1] C. Kalbach, Phys. Rev. C **37**, 2350 (1988).
[2] L. S. Azhgirey, I. K. Vzorov, V. P. Zrelov, M. G. Mescheryakov, B. S. Neganov, R. M. Ryndin, and A. F. Shabudin, Nucl. Phys. **13**, 258 (1959).
[3] N. S. Wall and P. R. Roos, Phys. Rev. **150**, 811 (1966).
[4] R. E. Chrien, T. J. Krieger, R. J. Sutter, M. May, H. Palevsky, R. L. Stearns, T. Kozlowski, and T. Bauer, Phys. Rev. C **21**, 1014 (1980).
[5] G. F. Bertsch and O. Scholten, Phys. Rev. C **25**, 804 (1982).
[6] J. M. Moss, T. A. Carey, J. B. McClelland, N. J. DiGiacomo, S. J. Seestrom-Morris, G. F. Bertsch, O. Scholten, G. S. Adams, M. Gazzaly, N. Hintz, and S. Nanda, Phys. Rev. Lett. **48**, 789 (1982).
[7] H. Esbensen and G. F. Bertsch, Phys. Rev. C **34**, 1419 (1986).
[8] C. Gaarde, J. Rapaport, T. N. Taddeucci, C. D. Goodman, C. C. Foster, D. E. Bainum, C. A. Goulding, M. B. Greenfield, D. J. Horen, and E. Sugarbaker, Nucl. Phys. **A369**, 258 (1981).
[9] J. Lisantti, J. R. Tinsley, D. M. Drake, I. Berqvist, L. W. Swenson, D. K. McDaniels, F. E. Bertrand, E. E. Gross, D. J. Horen, and T. P. Sjoreen, Phys. Lett. **147B**, 23 (1984).
[10] D. K. McDaniels, J. R. Tinsley, J. Lisantti, D. M. Drake, I. Berqvist, L. W. Swenson, F. E. Bertrand, E. E. Gross, D. J. Horen, T. P. Sjoreen, R. Liljestrand, and H. Wilson, Phys. Rev. C **33**, 1943 (1986).
[11] J. Lisantti, F. E. Bertrand, D. J. Horen, B. L. Burks, C. W. Glover, D. K. McDaniels, L. W. Swenson, X. Y. Chen, O. Häusser, and K. Hicks, Phys. Rev. C **37**, 2408 (1988).
[12] R. E. Segel, S. M. Levenson, P. Zupranski, A. A. Hassan, S. Mukhopadhyay, and J. V. Maher, Phys. Rev. C **32**, 721 (1985).
[13] C. Kalbach and F. M. Mann, Phys. Rev. C **23**, 112 (1981).
[14] A. A. Cowley, C. C. Chang, and H. D. Holmgren, Phys. Rev. C **22**, 2633 (1980).
[15] H. Machner, D. Protić, G. Riepe, J. P. Didelez, N. Frascaria, E. Gerlic, E. Hourani, and M. Morlet, Phys. Lett. **138B**, 39 (1984).
[16] R. E. Segel *et al.*, unpublished results quoted in Ref. 7.
[17] J. W. Wachter, W. A. Gibson, and W. R. Burrus, Phys. Rev. C **6**, 1496 (1972).
[18] S. M. Beck and C. A. Powell, NASA technical note NASA TN D-8119, National Aeronautics and Space Administration, Washington D.C., April 1976.
[19] D. M. Corley, N. S. Wall, H. Palevsky, J. L. Friedes, R. J. Sutter, G. W. Bennett, W. D. Simpson, G. C. Phillips, G. W. Igo, and R. L. Stearns, Nucl. Phys. **A184**, 437 (1972).
[20] M. M. Meier, D. B. Holtcamp, G. L. Morgan, H. Robinson, G. L. Russel, E. R. Whitaker, W. Amian, and N. Paul, in *Proceedings of the International Conference on Nuclear Data for Basic and Applied Science, Santa Fe, NM, 1985,* edited by P. Young *et al.* (Gordon and Breach, New York, 1985), Vol. II, p. 1647.
[21] J. R. Wu, C. C. Chang, and H. D. Holmgren, Phys. Rev. C **19**, 698 (1979).

[22]H. Machner (private communication).
[23]K. Chen, Z. Frankel, G. Friedlander, J. R. Grover, J. M. Miller, and Y. Shimamoto, Phys. Rev. **166**, 949 (1968).
[24]V. Flaminio, W. G. Moorhead, D. R. O. Morrison, and N. Rivoire, CERN Report No. CERN-HERA 84-01, 1984.
[25]Derek L. Livesey, *Atomic and Nuclear Physics* (Blaisdell, Waltham, MA, 1966), p. 373.
[26]R. G. Jeppesen, Ph.D. thesis, University of Colorado, 1986.
[27]Richard D. Smith and Michael Bozoian, Phys. Rev. C **39**, 1751 (1989).